International Journal of Trend in Scientific Research and Development (IJTSRD)
Volume 6 Issue 5, July-August 2022 Available Online: www.ijtsrd.com e-ISSN: 2456 – 6470

Transient Pressure Characterization of a Two-Stage Vertical Pump for Offshore Fire Suppression

Fareed Konadu Osman[1], Jinfeng Zhang[1], Israel Enema Ohiemi[1,2]

[1]National Research Center of Pumps, Jiangsu University, Zhenjiang, China
[2]Department of Mechanical Engineering, University of Nigeria, Nsukka, Nigeria

ABSTRACT

Off shore oil and gas installations are deliberately lifted considerably high above the water surface in order to prevent or reduce as much as possible the action of crashing waves and other marine phenomena. Pumps for firefighting on these installations need to be submerged in the water, but due to the height of the platforms, the available pumps struggled with inadequate lift and were unable to provide as much flow as needed. In this study, the original pump in operation which was originally designed to operate in single stage was combined into a two-stage pump and its performance was evaluated using experimental data from the single stage test as a benchmark. Further internal flow analysis of the transient pressure characteristics was conducted to understanding the key areas of pressure pulsations within this pump. This will serve as guide to conducting a multi-objective optimization of the multi-stage pump to subsequently improve the performance and prolong the operational lifespan.

KEYWORDS: *Vertical fire pump; Numerical simulation; Pressure Pulsations, Pump Performance Multistage*

How to cite this paper: Fareed Konadu Osman | Jinfeng Zhang | Israel Enema Ohiemi "Transient Pressure Characterization of a Two-Stage Vertical Pump for Offshore Fire Suppression" Published in International Journal of Trend in Scientific Research and Development (ijtsrd), ISSN: 2456-6470, Volume-6 | Issue-5, August 2022, pp.270-279, URL: www.ijtsrd.com/papers/ijtsrd50446.pdf

IJTSRD50446

1. INTRODUCTION

As a typical large-flow and high-head pump, the vertical pump has the characteristics of strong applicability, quick start and robust structure, so it is widely used in steel works, mines, water companies, power plants, sewage treatment plants and other enterprises, as well as flood control and drainage, offshore platforms, municipal water supply and drainage. In developed countries such as the United States, vertical long-shaft pumps are usually installed on offshore platforms as fire pumps. A recent increase in domestic offshore rigs, crude oil development platforms, large docks and other projects, have made vertical fire pumps more desirable for use in these projects[1,2].

Off shore oil and gas installations are deliberately lifted considerably high above the water surface in order to prevent or reduce as much as possible the action of crashing waves and other marine phenomena. Pumps for firefighting on these installations need to be submerged in the water, but due to the height of the platforms, the available pumps struggled with inadequate lift and were unable to provide as much flow as needed. Therefore, firewater pumps with vertically installed turbines on the shaft became the normal implementation as an extension of onshore well pumps [3].

Based on the analysis of existing literature, domestic research on the vertical fire pump with large flow and high head started relatively late. Wu Haiwei et al.[4] proposed in 2009 that the vertical long-shaft fire pump should replace the commonly used electric submersible pump as the seawater lift pump of offshore oil platform. Yu Kui et al.[5] analyzed the advantages of a vertical long-shaft fire pump in engineering use in 2009. Li Fuxing et al. [3] briefly analyzed the technical characteristics of a vertical long-shaft fire pump on offshore platforms in 2018. However, in China, although there are many manufacturers that develop and produce vertical long-shaft pumps (deep well pumps, condensate pumps,

chemical submersible pumps, etc.), the existing pump specifications are too small to meet the requirements of large flow and high head water supply in large fire engineering.

In a quest to improve the hydraulic design of multi-stage pumps, a lot of studies have been conducted both numerically through computer simulations and also through experimental procedures. These multistage pumps over the years have been mostly centrifugal and mixed-flow pumps. Numerical investigations of pressure fluctuations and rotor-stator interactions have been done over the years on several multi-stage vertical pumps in several number of pump and guide vane configurations[6–11].

Wang Wenjie[12] and Si Huang[13] conducted numerical simulations and predicted the performance in multi-stage submersible centrifugal pump. They discovered that the relative velocity flow angle and the absolute velocity flow angle are both reduced with the increasing of flow rate. They also concluded that the gap of impellers and diffusers is a point in the pump where high turbulent zones occur.

Minoru et al in 2017 studied the effects of viscosity on the flow characteristics of a multi-stage pump operating under submerged environment and found out that turbulence produced within the impeller region can be transported downstream to the diffuser, and recirculation from the diffuser can create negative flow effects into the next stage impeller. This phenomenon results in a substantial change in performance and flow pattern between the first and subsequent stages [14].

Chuan Wang in 2018 [15] conducted studies on the effects of pressure fluctuation, vibration, and noise on a multi-stage pump with radial diffuser by employing both numerical and experimental studies. At the end of the study, they concluded that rotor-stator-interactions create highly unsteady and potent pressure pulsations, vibration and noise, which makes the pump produce serious vibration and cause the corresponding noise. He also suggested that interstage pulsations in could cause irregular radial forces which could lead to vibrations and damage.

In 2019, Chuan et al[16] again conducted another numerical study on pressure fluctuation of a multi-stage centrifugal pump, but this time the scope was based on the whole flow field of the pump. They concluded that the inlet part of the outward diffuser pressure was the point of origin of the pressure fluctuations. Another point of origin of pressure fluctuation was the outlet side of the impeller blade.

In this study, the original pump in operation which was originally designed to operate in single stage will be combined into a two-stage multistage pump and its performance shall be evaluated using experimental data from the single stage test as a benchmark. Further internal flow analysis of the transient pressure characteristics. Understanding the key areas of pressure pulsations within this pump will serve as guide to conducting a multi-objective optimization of the multi-stage pump to subsequently improve the performance and prolong the operational lifespan.

2. Geometry and design parameters

Fig 1 displays the 3-D structure of the two-stage vertical pump. The pump is composed of six main components namely inlet pipe, outlet pipe, two impellers and two guide vanes.

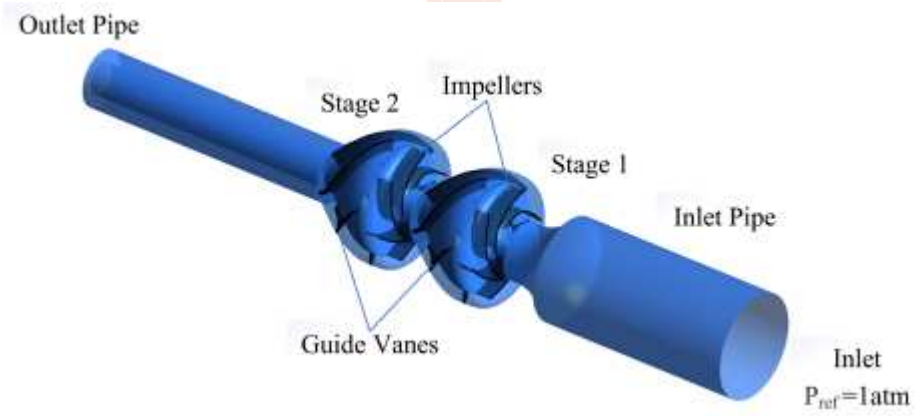

Fig 1. 3-D vertical pump model

Table 1. Design specifications of the pump

Parameter	Value
Rated Flow rate	240 (L/s)
Rated Head	81.2 (m)
Rotational speed	1485 (r/min)

Number of Impellers	2
Number of guide vanes	2
Number of Impeller blades	6
Number of guide vane blades	5

3. Numerical Modeling

3.1. Governing Equations

The Reynolds Averaged Navier-Stokes (RANS) equations, as well as the mass conservation and turbulent viscosity models, govern the flow. The fluid flow is considered to be incompressible, turbulent and three-dimensional for the sake of this analysis.

$$\frac{\partial u_i}{\partial x_i} = 0 \tag{1}$$

$$\rho\left[\frac{\partial \overline{u}_i}{\partial t} + \frac{\partial(\overline{u}_j \overline{u}_i)}{\partial x_j}\right] = \frac{\partial}{\partial x_j}\left[\mu\left(\frac{\partial \overline{u}_i}{\partial x_j}\right) - \rho\overline{u'_j u'_i}\right] - \frac{\partial \overline{p}}{\partial x_i} \tag{2}$$

Here, the Reynolds stress tensor is expressed as: - $\overline{\rho u_i' u_j'}$

$$-\rho\overline{u'_j u'_i} = \mu_t\left(\frac{\partial \overline{u}_j}{\partial x_i} + \frac{\partial \overline{u}_i}{\partial x_j}\right) - \frac{2}{3}\delta_{ij}\left(\rho k + \mu_t \frac{\partial \overline{u}_k}{\partial x_k}\right) \tag{3}$$

δ_{ij} is the Kronecker delta, $\delta_{ij} = \begin{cases} 1 \text{ for } i = j \\ 0 \text{ for } i \neq j \end{cases}$ $i, j = 1, 2, 3$

The turbulence model used was the shear stress transport (SST) k-ω model which is a blend of two models. It consists of the standard k-ω and k-ε equations which automatically shifts from near wall layers to free-stream flows. Menter[17,18] expressed the transport equations for turbulent kinetic energy and its dissipation rate for the SST k-ω model.

3.2. Grid Independence Analysis

The flow domain is in five main parts as illustrated in figure 2 below. In the mesh overview, only one of the impellers and one of the guide vanes are displayed. This is because they are identical in both stages of the pump. Details of the grid includes grid information of both impellers as shown in table 2 below. The grid independence analysis was conducted by following the method employed in the work of Celik et al.[19].

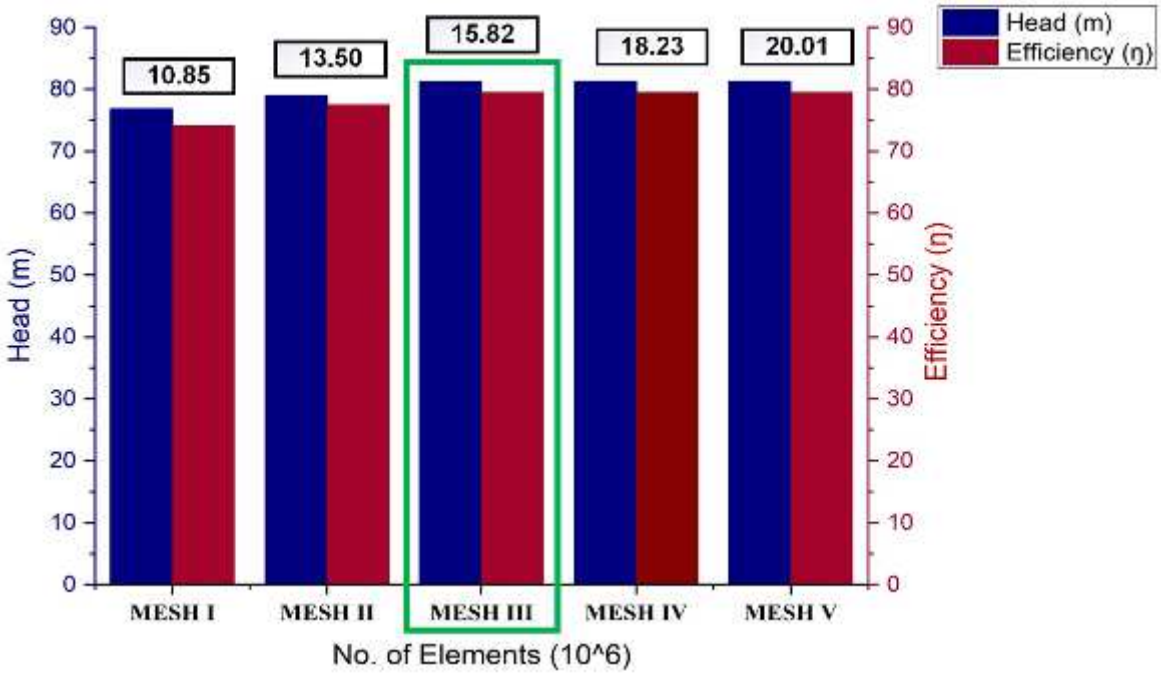

Fig 2. Performance of Independent Grids

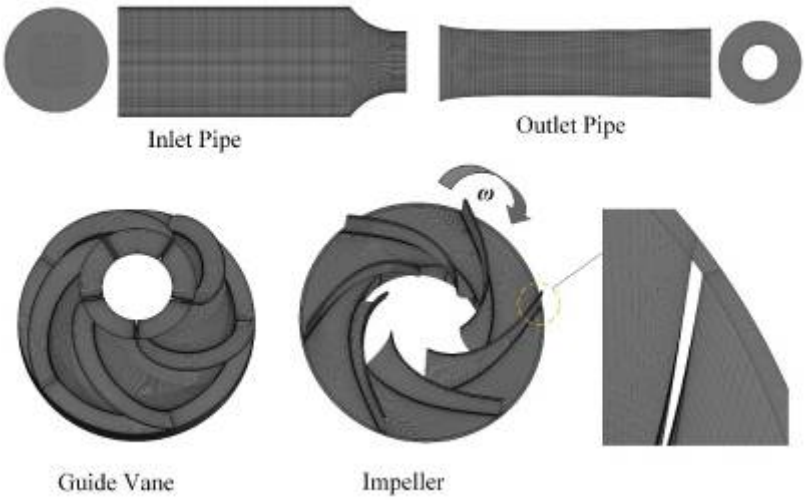

Fig 3. Mesh overview of the flow domain

Table 2. Grid details of flow domains

Domain	Impeller	Guide Vane	Guide Ring	Inlet	Outlet	Total
Pump	3428460 (2x)	3276810(2x)	215384(2x)	916080	1062936	15820324

3.3. Numerical Simulation Setup

The numerical calculations in this paper are done using ANSYS-CFX software. The detailed boundary conditions that were set to govern the numerical simulation has been outlined in table 3.

Table 3 Boundary conditions

Boundary Conditions	Settings
Turbulence Model	SST *k-ω*
Interface Configuration	Transient rotor-stator (Unsteady state)
Timestep	1.12235×10^{-4} s
Reference Pressure	101325 Pa = 1 atm
Inlet Condition	Total Pressure = 101325 Pa / 1 atm
Outlet Condition	Mass flow rate = 240 kg/s
Turbulence Intensity	Medium (5%) at inlet
Wall Roughness	Smooth wall
Shear Condition	No slip
Convergence Criterion	10^{-6}

Fig 3 depicts the location of the monitoring points within the computational domain of the pump. IMP represents points within the flow channels of the impeller and GV represents points within the flow channels of the guide vane.

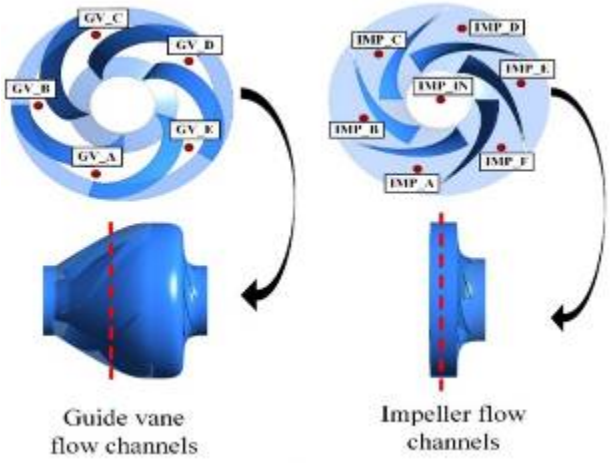

Fig 4 Monitoring points

3.4. Experimental Setup

An illustration of the experimental setup is depicted in Fig 4. The experiments were performed in accordance with the GB/T3216-2016. The tests were carried out at the rated rotational speed for several operating

conditions. The performance characteristics such as efficiency and pressure head of pump were thereafter, according to basic pump theory [20]. An illustration of the experimental setup is depicted in Fig 4.

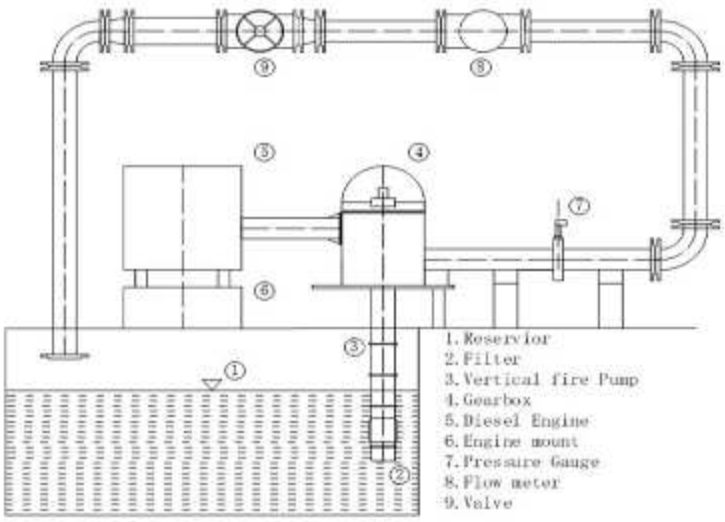

Fig 5 Diagram of Experimental Setup

3.5. CFD validation

A comparative analysis of the hydraulic performance curves between the experimental test and simulation results of the single stage pump was conducted which can be seen in Fig 5. For a level comparison, only the first stage of the simulated multistage pump, was used to compare the experimental results. The experimental and numerical values show good agreement for all three performance parameters. Under the rated working condition of $1.0Q_d$, the shaft power error was 1.5%, efficiency error was 4.65% and head error was 3.8%. In addition, the shaft power in the test and numerical calculation showed a trend of increasing with the increase of flow, indicating that there is a risk of motor power overload.

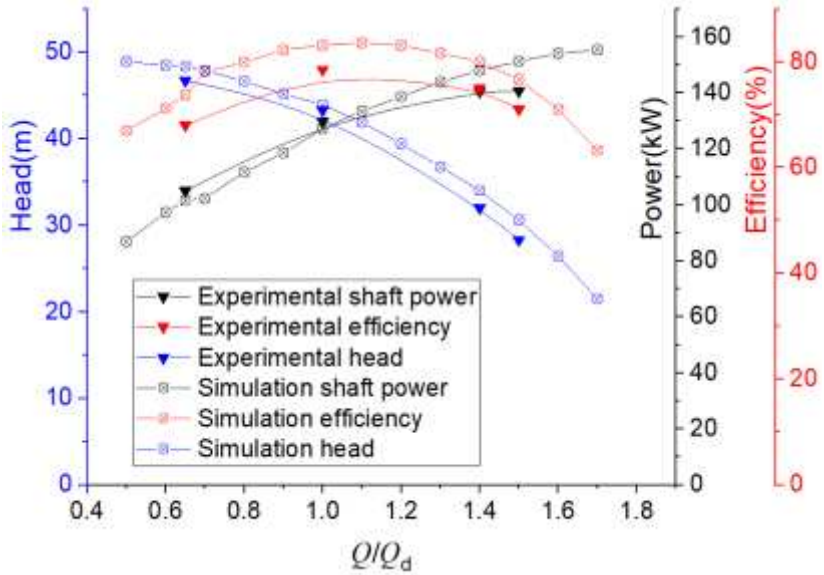

Fig 6 Performance Characteristics of experiments against simulation of 1st stage pump

4. Internal Pressure Pulsation Analysis of the Multi-stage Pump

Rotor-Stator-Interaction RSI has a major influence in characterization of transient flow in pumps. It has the tendency of generating strong pressure pulsations between the moving and stationary parts of the pump during operation. In order to properly examine the dynamic interactions that occur, it is imperative to monitor the stability of the pumps. Monitoring points have been placed within areas of interest of the pump. These areas are the impeller flow channels and the guide vane. The monitoring points record precise minute pressure fluctuations during the operation of the pump, however the ratio of the pressure changes at the monitoring points to the absolute value of the pressure value at that point is very small, therefore in order to make the pressure values simple and more convenient to work with, the dimensionless pressure coefficient C_p is introduced. The calculation formula of C_p is shown in Eqn. (4) below.

$$C_p = (p_i - \overline{p}) / (0.5\rho u_2^2) \quad (4)$$

Where: p_i (Pa) denotes the instantaneous pressure of the monitoring point, $\overline{p}$ (Pa) is the mean value of all pressure data recorded at the monitoring point, u_2 (m/s) is the outlet circumferential velocity of the blade and ρ (kg/m^3) is the density of fluid. The recorded pressure pulsation data were processed using the Fast Fourier Transform (FFT) into time domain and frequency domains. The pressure pulsation coefficient (C_p) is plotted at the design point ($1.0Q_d$) and overload flow conditions ($1.5Q_d$) at the aforementioned monitoring points.

4.1. Time Domain Analysis of Pressure Pulsations

A. Impeller Domain

This section depicts the time domain history of the pressure fluctuation coefficient within the pump impeller domain at both flow rates. The impeller domain is divided into the inlet, flow channels, pressure side of blades and the suction sides of the blades. Figs. 6 and 7 depict the time domain history of C_p at $1.0Q_d$ and $1.5Q_d$ in impeller flow passages of all stages of the pump. IMP1 and IMP2 represent the impellers in the stages of the pump. The attached alphabets A-F refers to the six flow channels within the impeller.

At $1.0Q_d$, for all stages, the graph depicted five peaks and five valleys which correspond to the number of blades in the guide vane. This is a clear depiction of rotor-stator influence as the stationary guide vane and the rotating impeller affects the pressure pulsations within the impeller. Considering the trends of the pulsations, it is seen that the C_p values increased with each stage since the absolute pressure increases from one stage to another.

At $1.5Q_d$, the waveforms for the second stage appear to have two troughs which indicate instability; however, they generally reflect the RSI influence that the guide vane blades have on the impeller pressure fluctuations. Considering the amplitudes of the pulsations at stages, it was seen that they increased with the progression in stages. This means that each stage is affected by the RSI excitation from the previous stage, which adds up to its own excitation and thus increasing it significantly.

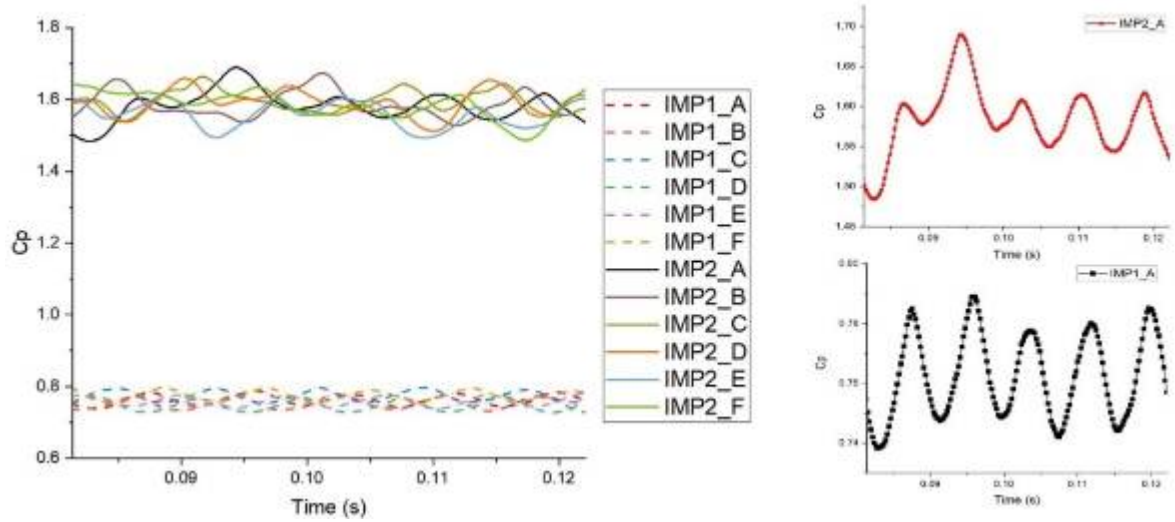

Fig 7. Time domain history of Cp at 1.0Qd in impeller flow passage

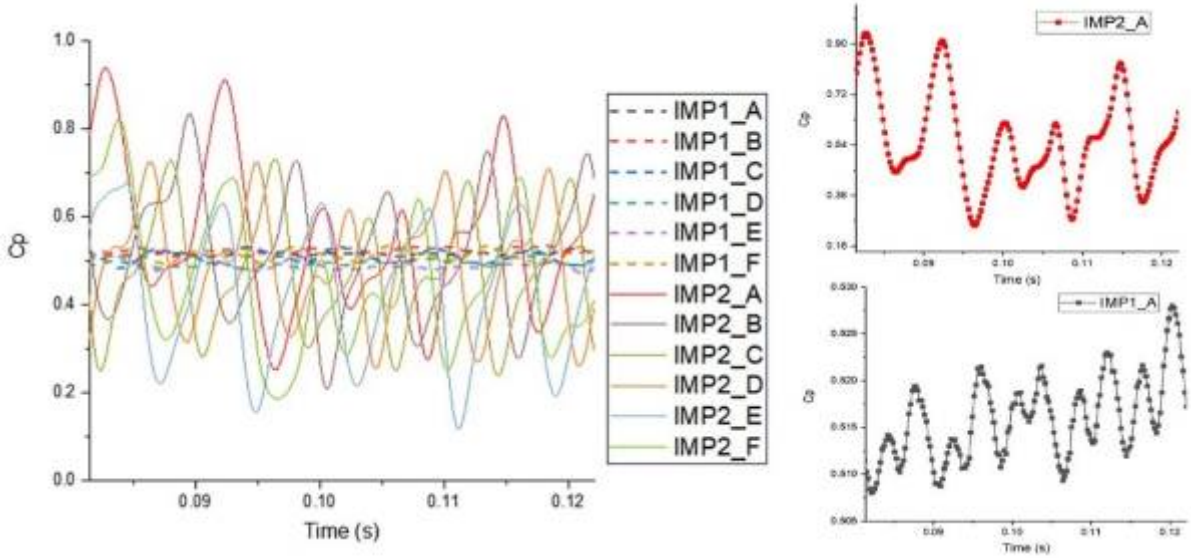

Fig 8. Time domain history of Cp at 1.0Qd in impeller flow passage

B. Guide Vane Domain

This section depicts the time domain history of the pressure fluctuation coefficient within the guide vanes at both flow rates. The guide vane of this pump is the point where most of the swirling flow from the impeller is channeled axially and then diffused to increase overall head.

Figs. 8 and 9 depicts the C_p distribution within the Guide Vane. GV1 and GV2 represent the guide rings in the first and second stages respectively and alphabet designations A-E refers to each of the six impeller outlets. At design flow condition of $1.0Q_d$ flow condition in the first stage, the waveform of the pulsations had irregular periodicity and fails to clearly depict the six peaks that corresponds to the number of impeller blades. The C_p trend ranged between 1.09~1.11 for the first stage, 1.95~2.1 in the second stage. However, at the large flow rate of $1.5Q_d$, the waveforms in all stages still depicted obvious periodicity. The amplitudes of C_p trends were similar to that of the design flow condition.

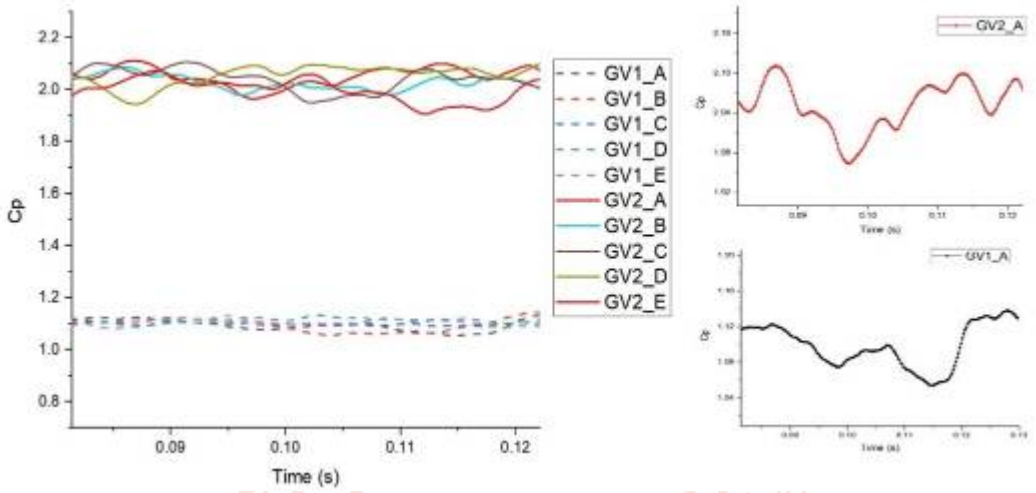

Fig 9 Time domain history of Cp at 1.0Qd in guide vane

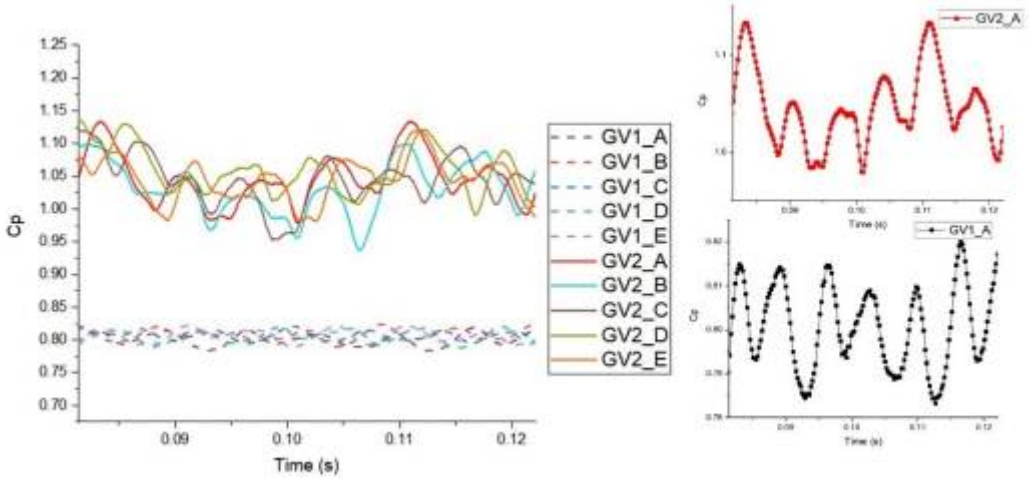

Fig 10 Time domain history of Cp at 1.5Qd in guide vane

4.2. Frequency Domain Analysis of Pressure Pulsations

A. Impeller Domain

This section discusses the frequency-domain history of the monitoring points in the impeller flow passage. This was attained by using the Fast Fourier Transform (FFT) analysis of the values recorded by the monitoring points in the domain under investigation. The pressure intensity amplitudes are mainly subjected to shaft frequency, f_n and frequency excitations. With the impeller rotational speed at 1485 r/min, the shaft frequency occurs at 24.75 Hz while the excited frequencies usually occur at multiples of the shaft frequency.

Fig 10 and Fig 11 show the frequency domain C_p within the impeller flow passage. The frequencies excited by pressure fluctuation occurred at 123.75 Hz ($5 \times f_n$), 247.5 Hz ($10 \times f_n$), and 371.25 Hz ($15 \times f_n$) for all monitoring points at both design and overload flow conditions. Within the impeller flow channels, the main frequency has a value of 123.75 Hz which is five times the impeller frequency which corresponds to the number of guide vane blades. This means that the pulsations causing the excitation are influenced by the interaction between the guide vane and the impeller. On the impeller blades as depicted in Figs. 4.18 and 4.19, the pressure fluctuation amplitudes continue to increase at all the monitoring points as we move from the inlet of the pump, through the

stages and towards the outlet with the IMP1 monitors recording the lowest fluctuations and IMP3 records the highest.

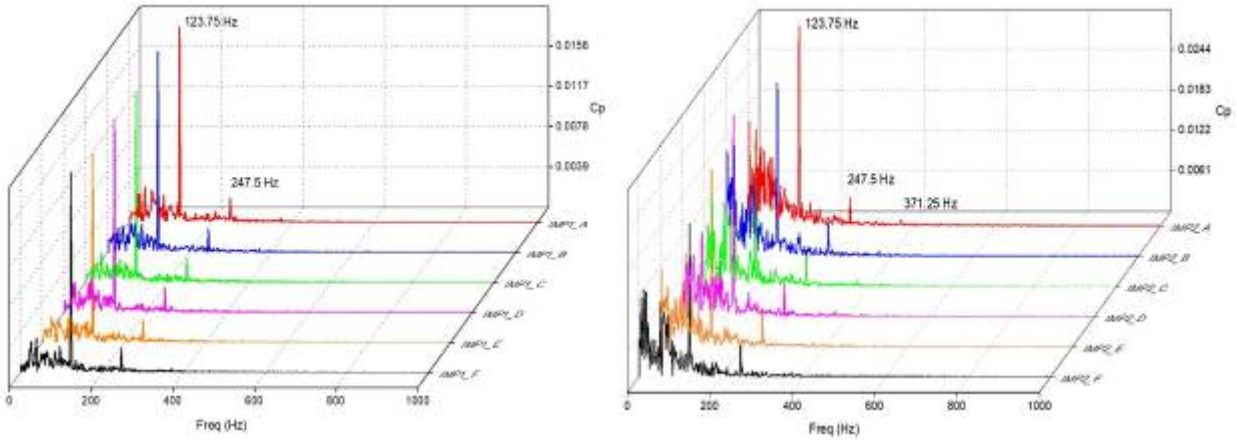

(a)Stage 1 **(b) Stage 2**

Fig 11 Frequency domain history at 1.0Qd in impeller flow passage

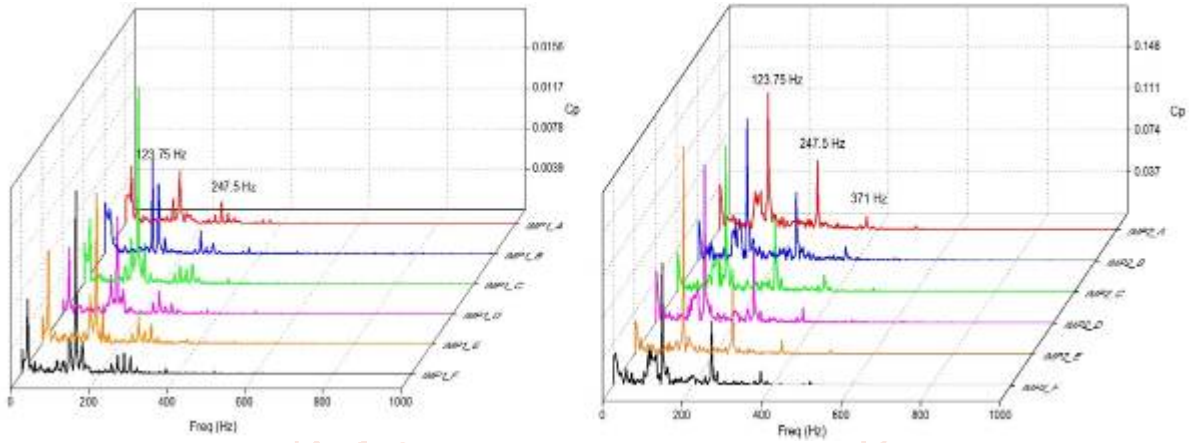

(a)Stage 1 **(b) Stage 2**

Fig 12 Frequency domain history at 1.5Qd in impeller flow passage

B. Guide Vane Domain

The frequency-domain history of the monitoring points in the guide vane is shown in Figs. 12 and 13. The frequencies excited by pressure fluctuation occurred at 148.5 Hz ($6 \times f_n$) and 297 Hz ($12 \times f_n$). In the stage 2 guide vanes channels, there appear to be influence of pulsations which do not occur at the shaft frequency or any of its harmonics, but still present significant amplitudes. These could be attributed to the fact that there are differences within the frequency distributions in both impellers and both guide vanes of the previous stages and these propagate into the last stage of the pump and causes that phenomenon. However, the main excitation effect due to harmonics recorded across all the monitoring points is the consequences of flow exchange between the guide vane and the impeller, which is overall dependent on impeller blade number. The amplitude was also found to decrease with the increase in flow rate across all flow conditions.

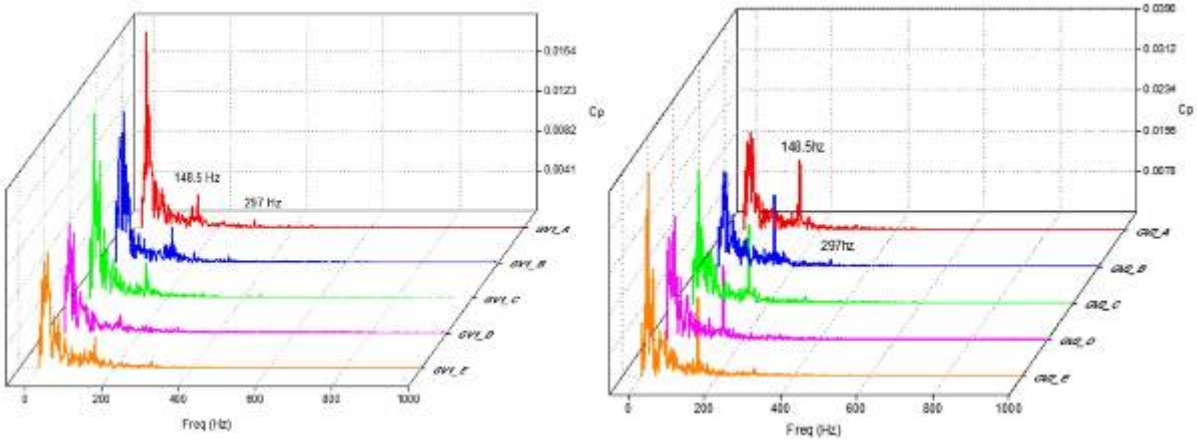

(a)Stage **1 (b) Stage 2**

Fig 13 Frequency domain history at 1.0Qd in guide vane

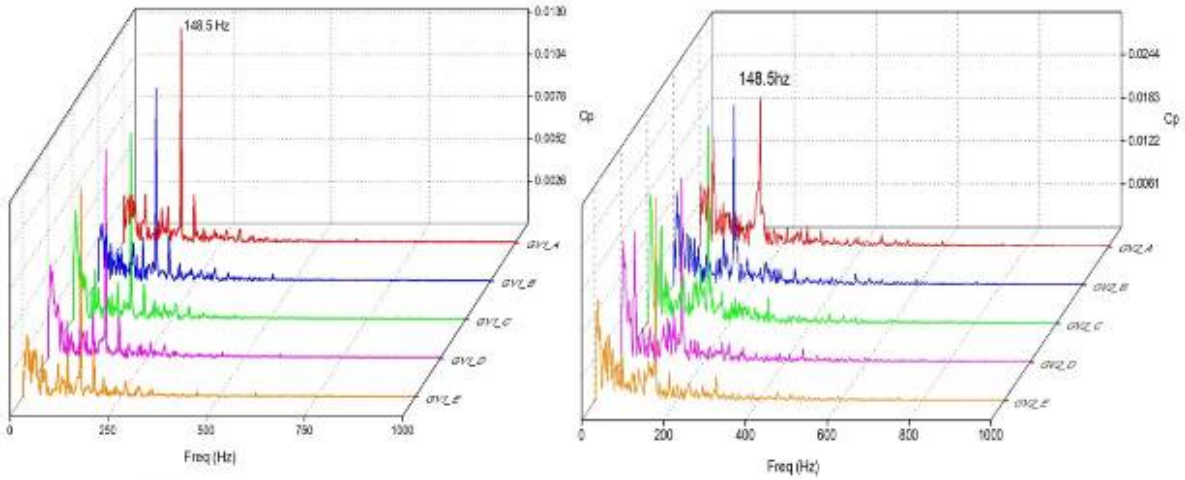

(a)Stage 1 **(b) Stage 2**

Fig 14 Frequency domain history at 1.0Qd in guide vane

5. Conclusion

In this study, the unsteady pressure fluctuations generated from the operation of the multi-stage pumps at design and overload conditions were analyzed. Through careful studies of the flow characteristics in the pump under different timesteps, the locations and reasons for the poor hydraulic performance of the pump are well established and following remarks are reached:

A. The pressure pulsations generated within the pump is caused by the rotor-stator interaction between the rotating parts and the stationary parts.
B. Pressure pulsation exists in three forms: white noise, blade frequency and shaft frequency. White noise pressure pulsation exists in the inlet section of the first stage of the pump.
C. It is observed that the number of blades in the impellers and guide vanes have a strong influence on the peak pressure fluctuations. The blade number also influences the frequency at which these peak fluctuations occur.
D. Also, it was observed that the amplitudes of the harmonics of the frequencies are not the same. They tend to reduce as the harmonics increase.
E. Finally, within the final stage stage of the multistage pump, there was an influence of pulsations which did not occur exactly at the shaft frequency or any of its harmonics, but still present significant amplitudes. This was attributed to excitations of the different parts of the pump that propagated from the lower stages.

ACKNOWLEDGEMENTS

This work was supported by the Primary Research & Development Plan of Jiangsu Province (Grant no. BE2019009-1). The authors declare no competing financial interests.

NOMENCLATURE

P	pressure, Pa
H	head, m
Q	flow rate, m^3/h
η	efficiency
n	rotational speed, r/min
ω	angular speed, rad/s
ρ	density, kg/m^3
t	time, s
g	gravity, m/s^2
$-\rho\overline{u_i'u_j'}$	Reynolds-stress tensor
k	kinetic energy of turbulence, m^2/s^2
ω	specific dissipation of turbulence kinetic energy, s^{-1}
ε	dissipation of kinetic energy of turbulence, m^2/s^3
C_μ	Constant
μ_t	turbulent viscosity, m^2/s
δ_{ij}	Kronecker delta

Subscript

i, j	components in different directions
x_i	cartesian coordinates: x, y, z

Abbreviations

CFD	Computational Fluid Dynamics
RANS	Reynolds-averaged Navier-Stokes equations
SST	Shear Stress Transport

References

[1] J. Zhang, Z. Yang, L. Lai, H. Song, C. Jing, Automatic Optimization of Vertical Long-shaft Fire Pump Overload Based on Particle Swarm Optimization Algorithm, in: IOP Conf. Ser. Mater. Sci. Eng., IOP Publishing, 2021: p. 12017.

[2] Q. Si, S. Yuan, C. Wang, B. Hu, "Optimal design of submersible multistage pumps with low specific speed," Trans. Chinese Soc. Agric. Eng. 28 (2012) 122–127.

[3] F. Li, "Analysis of Technical Characteristics of Vertical long shaft Fire Pump in Offshore Platform," Intern. Combust. Engine Accessories. 38 (2018) 67~68.

[4] Y.Z. Wu Haiwei, Liu Qiguang, "Problems and Alternatives of electric submersible pump used as Seawater Lift pump for offshore Oil Platform.," China Pet. Chem. Stand. Qual. 38 (2018) 138~139.

[5] K. Yu, "Analysis of the characteristics of vertical long-axis fire pumps.," First Natl. Conf. Fire Prot. Supertall Build. (2014).

[6] W. Li, X. Jiang, Q. Pang, L. Zhou, W. Wang, "Numerical simulation and performance analysis of a four-stage centrifugal pump," Adv. Mech. Eng. 8 (2016) 1687814016673756.

[7] L. Zhou, W. Shi, L. Bai, W. Lu, W. Li, Numerical investigation of pressure fluctuation and rotor-stator interaction in a multistage centrifugal pump, in: Fluids Eng. Div. Summer Meet., American Society of Mechanical Engineers, 2013: p. V01BT10A029.

[8] C. Yang, X. Cheng, Numerical simulation of three-dimensional flow in a multistage centrifugal pump based on integral modeling, in: 2009 Asia-Pacific Power Energy Eng. Conf., IEEE, 2009: pp. 1–5.

[9] S. Huang, A.A. Mohamad, K. Nandakumar, Z.Y. Ruan, D.K. Sang, "Numerical simulation of unsteady flow in a multistage centrifugal pump using sliding mesh technique," Prog. Comput. Fluid Dyn. An Int. J. 10 (2010) 239–245.

[10] A.E. Khalifa, A.M. Al-Qutub, R. Ben-Mansour, "Study of pressure fluctuations and induced vibration at blade-passing frequencies of a double volute pump," Arab. J. Sci. Eng. 36 (2011) 1333–1345.

[11] L. Bai, L. Zhou, C. Han, Y. Zhu, W. Shi, "Numerical study of pressure fluctuation and unsteady flow in a centrifugal pump," Processes. 7 (2019) 354.

[12] W.J. Wang, G.D. Li, Y. Wang, Y.R. Cui, G. Yin, S. Peng, Numerical simulation and performance prediction in multi-stage submersible centrifugal pump, in: IOP Conf. Ser. Mater. Sci. Eng., IOP Publishing, 2013: p. 32001.

[13] S. Huang, M.F. Islam, P. Liu, "Numerical simulation of 3D turbulent flow through an entire stage in a multistage centrifugal pump," Int. J. Comut. Fluid Dyn. 20 (2006) 309–314. https://doi.org/10.1080/10618560600916981.

[14] E.M. Ofuchi, H. Stel, T. Sirino, T.S. Vieira, F.J. Ponce, S. Chiva, R.E.M. Morales, "Numerical investigation of the effect of viscosity in a multistage electric submersible pump," Eng. Appl. Comput. Fluid Mech. 11 (2017) 258–272.

[15] C. Wang, X. Chen, N. Qiu, Y. Zhu, W. Shi, "Numerical and experimental study on the pressure fluctuation, vibration, and noise of multistage pump with radial diffuser," J. Brazilian Soc. Mech. Sci. Eng. 40 (2018) 1–15.

[16] C. Wang, X. He, W. Shi, X.X. Wang, X.X. Wang, N. Qiu, X. Gong, J. Pei, W. Wang, M.K. Osman, W. Jiang, J. Zhao, Q. Deng, "Numerical study on pressure fluctuation of a multistage centrifugal pump based on whole flow field," AIP Adv. 9 (2021) 771.

[17] F.R. Menter, "Two-equation eddy-viscosity turbulence models for engineering applications," AIAA J. 32 (1994) 1598–1605.

[18] F. Menter, Zonal two equation kw turbulence models for aerodynamic flows, in: 23rd Fluid Dyn. Plasmadynamics, Lasers Conf., 1993: p. 2906.

[19] I.B. Celik, U. Ghia, P.J. Roache, C.J. Freitas, "Procedure for estimation and reporting of uncertainty due to discretization in CFD applications," J. Fluids Eng. ASME. 130 (2008).

[20] J.F. Gulich, "Centrifugal Pumps, Springer," Berlin, Ger. (2008).